

Interpretation of Carbonyl Band Splitting Phenomenon of a Novel Thermotropic Liquid Crystalline Polymer without Conventional Mesogens: Combination Method of Spectral Analysis and Molecular Simulation

Shengtong Sun, Hui Tang, and Peiyi Wu*

Key Laboratory of Molecular Engineering of Polymers, Ministry of Education, Department of Macromolecular Science, and Laboratory of Advanced Materials, Fudan University, Shanghai 200433, People's Republic of China

Received: September 16, 2009; Revised Manuscript Received: December 19, 2009

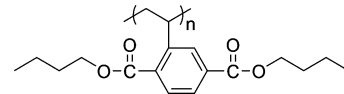
A combination method of spectral analysis and molecular simulation was employed to interpret the carbonyl band splitting phenomenon of poly[di(butyl)vinylterephthalate] (PDBVT), a novel thermotropic liquid crystalline polymer, which can self-assemble into a two-dimensional hexagonal, columnar ($2D \Phi_H$) phase without conventional mesogens. Two-dimensional correlation infrared spectroscopy results of PDBVT during heating showed four splitting bands at 1707, 1712, 1731, and 1741 cm^{-1} . Accordingly, four PDBVT conformers were classified on the basis of carbonyls rotating in a π -electron resonance system. Detailed spectral comparison and molecular dynamics (MD) simulation for the columnar phase of PDBVT were carried out to make a clear assignment of splitting bands to different conformers. The internal self-assembly nature of PDBVT can be concluded that the rotation of carbonyls at the 2-position (close to backbone) of the phenylenes would take place, along with the formation of the $2D \Phi_H$ phase. Meanwhile, the consecutive motions of PDBVT backbones with a distortion and extension in the mesophase formation and preparation processes have also been examined and reproduced by MD simulation. Finally, a good simulated conformity of the side chain size dependence of the liquid crystallinity of PDAVTs with experimental observations was achieved. This work combining spectral analysis and molecular simulation may bring some new insight into a better understanding of various physical chemical phenomena unintelligible before.

1. Introduction

Combining properties of a high molecular mass and a liquid crystalline phase, liquid crystalline polymers (LCPs) have been well-known for their excellent anisotropic physical properties, easy processing, and convenient molecular tailoring.¹ Generally, LCPs have some rigid groups or mesogens in their structure units to generate liquid crystallinity, either for main chain or side chain LCPs. But this is not always necessary. Derived from traditional mesogen-jacketed LCPs (MJLCPs),² poly[di(alkyl)vinylterephthalate]s (PDAVTs)^{3–5} are one of rare some LCPs (others such as polyphosphazenes,^{6,7} poly(di-*n*-alkylsiloxane)s,^{8,9} et al.) that can exhibit unexpected thermotropic liquid crystallinity without conventional mesogens. In PDAVTs, the rigidity of the pendent side groups is extremely weakened by incorporating linear alkyl groups into the 1,4-phenylene groups through ester linkages. No obvious mesophase transition of PDAVTs could be observed during DSC heating and cooling experiments except for the glass transition.³ Further investigation showed that PDAVTs could develop into a two-dimensional, hexagonal, columnar ($2D \Phi_H$) phase only if the linear alkyl groups are in an appropriate range (3–6 carbon chains), and too short or too long both resulted in the disruption of liquid crystallinity.⁴

In our previous work, we employed two-dimensional correlation infrared spectroscopy (2DIR) and a perturbation correlation moving window (PCMW) technique to elucidate the supramolecular self-assembly nature of PDBVT (Scheme 1, *B* = butyl).¹⁰ Largely different from traditional MJLCPs,¹¹ the backbones of PDBVT exhibited “extension–distortion–slight extension” consecutive motions in the whole self-assembly

SCHEME 1: Chemical Structure of PDBVT



process on a mesoscale, and carbonyl may be closely related to the formation of the $2D \Phi_H$ phase as the starting point of molecular motions upon heating. However, a detailed discussion about carbonyl influence on mesophase formation and the internal self-assembly nature of PDBVT has not been carried out. Interestingly, in the analyses of differential spectra and 2D synchronous/asynchronous spectra (as shown in Figures 2 and 5), carbonyl exhibited two and four splitting bands, respectively. This provided us very important information of subtle carbonyl conformational changes, which may be helpful to reveal the internal self-assembly nature of PDBVT. Nevertheless, two main problems limited our further investigation: how to classify different carbonyl conformers and how to assign them to corresponding splitting bands.

As we know, IR spectroscopy is very sensitive to morphology. Among the different bands used for spectral analysis, the carbonyl stretching band is undoubtedly the most important one as a relatively localized vibration mode that is almost uncoupled with the vibrations of the chain skeleton and usually well resolved in IR spectrum. But meanwhile, plenty of intra- and intermolecular interactions and conformational changes make this region even more complicated.¹² Consequentially, it brought on large difficulties for researchers to understand the origin of spectral components, but we could also extract much subtle information from it. Up to now, a similar carbonyl band splitting phenomenon has been found in many chemical systems,

* Corresponding author. E-mail: peiyiwu@fudan.edu.cn.

TABLE 1: The Molecular Weights, Thermal Properties and Liquid Crystallinity of Three PDBVT Samples

sample ID	M_n ($\times 10^{-4}$) ^a	PDI ^a	DP ^a	T_g (°C) ^b	liquid crystallinity	T_{LC} (°C) ^c
PDBVT-1	1.4	1.14	46	<−50	no	
PDBVT-2	2.3	1.23	76	−6	no	
PDBVT-3	9.4	1.31	309	0.6	yes	100

^a M_n , number average molecular weight; PDI, polydispersity index; DP, degree of polymerization, determined by GPC measurements with monodisperse polystyrene as standard and THF as eluent phase at 35 °C. ^b T_g , glass transition temperature, determined by the second heating DSC experiments. The T_g of PDBVT-1 is lower than −50 °C and cannot be precisely detected. ^c T_{LC} , mesophase transition temperature, determined by 1D WAXD measurements.

sometimes along with a slight band shift. For example, poly(L-lactide)s (PLLA)s are one of the most investigated polymers, whose carbonyl in ester bonds exhibited at least three splitting bands, in either the amorphous or crystalline phase. That carbonyl band splitting is so liable to occur arises from its being almost the largest dipole moment of all chemical bonds. Nowadays, different models have been proposed to explain changes of PLLA conformers in the crystallization process, such as crystal field splitting,¹³ mechanical coupling,¹⁴ transition dipole coupling,¹² intramolecular through bond coupling,¹⁵ interchain dipole–dipole interaction,^{16,17} and even specific H-bonding forces between C–H and C=O.¹⁸ In addition, the carbonyl band splitting phenomenon can also be found in polypeptides and proteins^{19–22} and some other carbonyl-containing copolymers.^{23,24}

Similarly, we can make a clear classification of carbonyl conformers of PDBVT based on the above carbonyl band splitting mechanisms. To further assign these splitting bands, a new molecular dynamics (MD) simulation method was employed in this paper. Nowadays, MD techniques are playing an important role in modern characterization of materials due to their excellent simplifying of complicated systems with “force field” files.^{25–27} Fortunately, 2D WAXD results of PDAVTs^{4,28} served many valuable structural parameters of the 2D Φ_H phase, which offered us many conveniences for the construction of the amorphous and columnar phase of PDBVT through MD simulation.

In this paper, we make a detailed spectral comparison among three different PDBVT samples with different molecular weights to examine the variations of carbonyl stretching profiles during heating. On the basis of classification and assignment of different carbonyl conformers, subtle chain conformational changes in the preparation and formation stages of the 2D Φ_H phase we have never discovered before were elucidated. Our new attempt to combine spectral analysis and molecular simulation methods may bring some new insight into a deep understanding of various physical–chemical phenomena hard to interpret before.

2. Experimental Methods

2.1. Materials. Three PDBVT samples of different molecular weight were synthesized via the atom transfer radical polymerization (ATRP) method. The molecular weights, thermal properties, and their liquid crystallinity are presented in Table 1. Therein, only PDBVT-3 whose molecular weight is higher than the critical molecular weight, can develop into the 2D Φ_H phase above phase transition temperature (~ 100 °C derived from WAXD measurements). No obvious mesophase transition of PDBVT-3 can be observed in DSC experiments except for the glass transition (~ 0.6 °C).

2.2. Investigation Methods. 2.2.1. FT-IR Spectroscopy.

PDBVT samples for FT-IR measurements were all prepared by a film casting method on a KBr tablet with tetrahydrofuran (THF) as the solvent. All time-resolved FT-IR spectra at different temperatures were recorded on a Nicolet Nexus 470 spectrometer with a resolution of 4 cm^{−1}, and 32 scans were available for an acceptable signal-to-noise ratio. Temperature-dependent spectra were collected between 40 and 160 °C with an increment of 5 °C. Raw spectra were baseline-corrected by the software Omnic, verison 6.1a.

2.2.2. 2D Correlation Spectroscopy. FT-IR spectra collected in the temperature range 40–160 °C with 5 °C interval were used to perform 2D correlation analysis. 2D correlation analysis was carried out using the software 2D Shige, verison 1.3 (Shigeaki Morita, Kwansei-Gakuin University, Japan, 2004–2005), and was further plotted into the contour maps by the Origin program, version 8.0. In the contour maps, red is defined as positive intensities; green, as negative intensities.

2.2.3. Perturbation Correlation Moving Window. FT-IR spectra used for 2D correlation analysis were also used to perform perturbation correlation moving window analysis. Primary data processing was carried out with the method Morita provided, and further correlation calculation was performed using the same software, 2D Shige, verison 1.3 (Shigeaki Morita, Kwansei-Gakuin University, Japan, 2004–2005). Similarly, the final contour maps were plotted by the Origin program, version 8.0, with the same colors defined as the same significations as 2D correlation analysis. An appropriate window size ($2m + 1 = 11$) was chosen to generate PCMW spectra with good quality.

2.2.4. Molecular Dynamics Simulation. All the molecular structures of repeat units and polymers in their amorphous and columnar phase were constructed in the software package Materials Studio, version 4.4 (Accelrys Inc., San Diego, CA, 2008). Therein, the amorphous phase of PDBVT was specially constructed in the Amorphous Cell module. The energy optimization and molecular dynamics run were accounted for by the COMPASS force field, which was implemented in the Forceite and Discover modules.

3. Results and Discussion

3.1. Spectral Comparison of PDBVT Samples with Different Molecular Weights. Our previous work showed that carbonyl may be closely related to the formation of the 2D Φ_H phase as the starting point of molecular motions upon heating.¹⁰ However, a precise description of their relationship has not yet been clarified, which limited our further comprehension of the internal self-assembly nature of PDBVT. Fortunately, there exists an interesting phenomenon that the liquid crystallinity of PDBVT is molecularly weight-dependent; that is, PDBVT has a critical chain length above which only the 2D Φ_H phase can be developed.⁵ It can be interpreted as not enough persistence length to stabilize the columnar phase due to relatively low chain length. Thus, it is reasonable to consider that whether the mesophase can be formed should bring some differences to carbonyl stretching variation profiles.

Three PDBVT samples were chosen to make the spectral comparison, whose molecular weight and thermal properties have been presented in Table 1. It is noteworthy that only PDBVT-3 can form the 2D Φ_H phase above the mesophase transition temperature (T_{LC} , ~ 100 °C), which is also the research object we discussed in our previous paper. In this paper, we are concerned with merely carbonyl conformational changes;

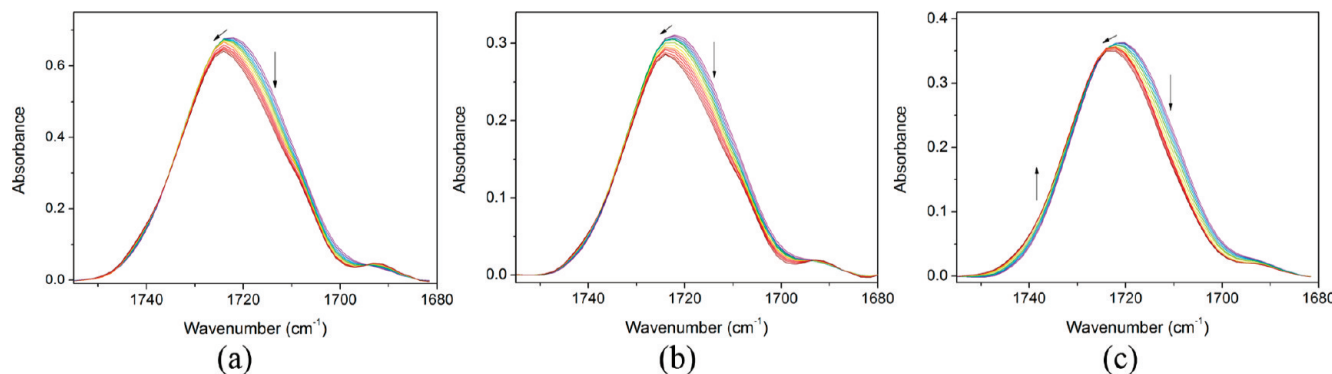


Figure 1. Conventional IR spectral variations in the region $1755\text{--}1680 \text{ cm}^{-1}$ during heating ($40\text{--}160^\circ\text{C}$) of three PDBVT samples (a, PDBVT-1; b, PDBVT-2; c, PDBVT-3). For clarity, only a 10°C interval is shown here.

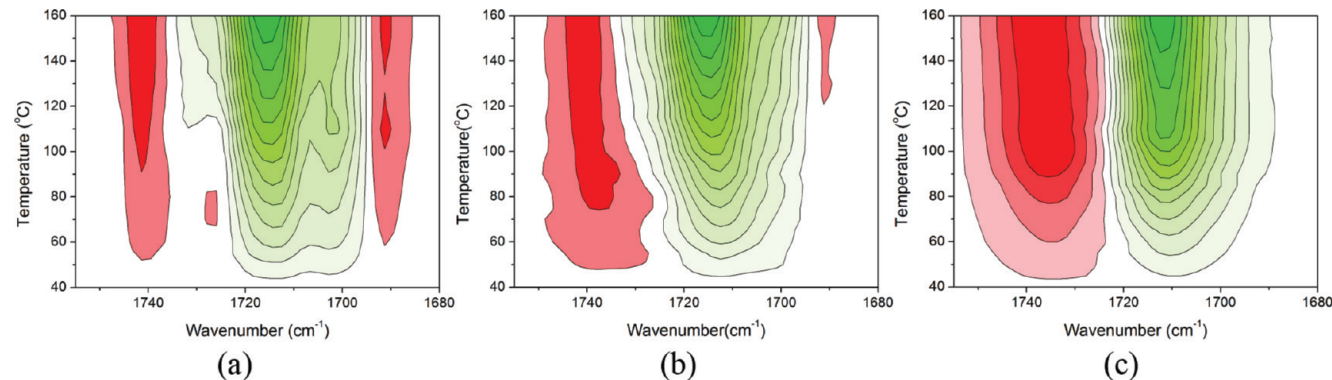


Figure 2. Contour maps of differential spectra in the region $1755\text{--}1680 \text{ cm}^{-1}$ during heating ($40\text{--}160^\circ\text{C}$) of three PDBVT samples (a, PDBVT-1; b, PDBVT-2; c, PDBVT-3). The spectrum collected at 40°C was used as the reference spectrum. Red is defined as intensity increasing; green, intensity decreasing.

thus, only the region $1755\text{--}1680 \text{ cm}^{-1}$ corresponding to the C=O stretching vibration was selected for performing a spectral comparison.

3.1.1. Conventional IR. Figure 1 shows the conventional IR spectral variations of the region $1755\text{--}1680 \text{ cm}^{-1}$ during heating ($40\text{--}160^\circ\text{C}$) of the three PDBVT samples. For clarity, only a 10°C interval is shown here. It is notable that a shoulder peak around 1698 cm^{-1} cannot be assigned to any fundamental vibrational modes (maybe an overtone of the deformation vibration of phenylene); thus, in this paper, we are inclined to attribute it to an interference peak, and no noticeable influence can be found on our later analyses.

At lower temperature, the spectrum profiles of these three samples are quite similar to each other. However, at higher temperature, PDBVT-1, and -2 exhibited a shoulder peak around 1707 cm^{-1} much more obviously than PDBVT-3. It is speculated that the carbonyl conformation corresponding to the band at 1707 cm^{-1} is favorable to the amorphous phase but unfavorable to the columnar phase. Carefully examine the three carbonyl stretching spectral variation tendencies during heating, and you can also find some remarkable differences. For PDBVT-3, there exist three main spectral changes: intensity increasing around the band at 1736 cm^{-1} , intensity decreasing around the band at 1710 cm^{-1} , and a slight peak shift to a higher wavenumber around the band at 1720 cm^{-1} . But for PDBVT-1 and -2, only the latter two spectral changes can be observed. It indicates that the carbonyl conformation corresponding to the band at 1736 cm^{-1} may have a large contribution to the formation of the 2D Φ_H phase. Especially noteworthy is that the peak shift of the C=O stretching band of PDBVT does not look like the result of a gradual shift of band position or a gradual change of the bond strength, but more like the result of the population changes

within the mixtures of different carbonyl conformations due to an obvious band shape changing during heating.^{29,30}

3.1.2. Differential Spectra. To examine spectral variations more directly, differential spectra of these three samples have also been plotted in Figure 2. The spectrum collected at 40°C was used as the reference spectrum. From differential spectra, we can get an obvious observation of two splitting peaks: the gradually growing band at 1736 cm^{-1} and the gradually disappearing band at 1705 cm^{-1} from PDBVT-1 to PDBVT-3. The preference of the band at 1736 cm^{-1} for the mesophase and that of the band at 1707 cm^{-1} for the amorphous phase were emphasized once again by differential spectra.

From the differential spectra, we found the band around 1710 cm^{-1} had the largest intensity variation degree. Therefore, we chose this band to examine the temperature dependence of carbonyl spectral intensity during heating. The absorbance variations of the band at 1710 cm^{-1} of these three samples as a function of temperature are presented in Figure 3. All the absorbance intensities have been normalized for the convenience of comparison. Interestingly, PDBVT-1 and -2, which cannot evolve into the mesophase at higher temperature, exhibited a nearly linear decrease in absorbance with an increase in temperature, whereas PDBVT-3 exhibited an anti-S-shaped decrease with an obvious turning point at 110°C owing to the finish of mesophase formation and the start of mesophase perfection, as we reported in our previous paper.¹⁰ Compare the total degree of decrease in absorbance as the temperature was increased from 40 to 160°C , and we can find that PDBVT-3 has the largest value ($\sim 26\%$). Temperature-dependent IR spectra of PDBVT presented a good reflection of its molecular weight dependence of the liquid crystallinity.

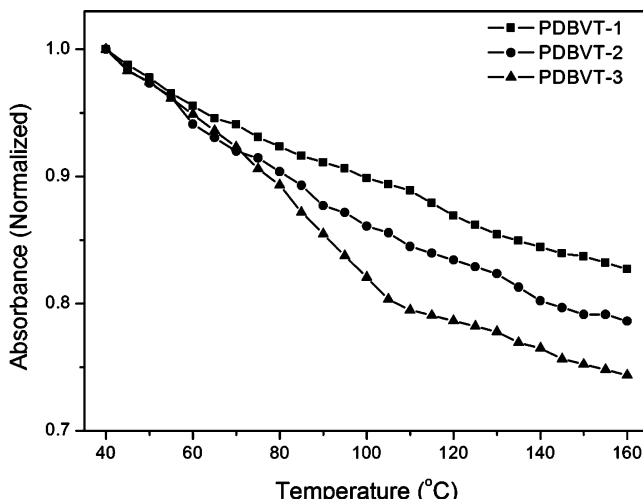


Figure 3. The absorbance (normalized) variations of the band at 1710 cm^{-1} of three PDBVT samples as a function of temperature.

3.1.3. Perturbation Correlation Moving Window. Perturbation correlation moving window³¹ is a newly developed technique that can be used to determine transition points and additionally monitor complicated spectral variations along the perturbation direction.

Figure 4 shows the PCMW synchronous and asynchronous spectra of three PDBVT samples generated from the whole spectra during heating (40–160 °C). PCMW synchronous spectra are very helpful in finding transition points, especially the weak mesophase transition of PDBVT, which cannot be detected by conventional thermal analysis. T_{LC} of PDBVT-3 can be easily read out to be ~85 °C (where the largest correlation intensity is located), approximately the result obtained from 1D WAXD (~100 °C). However, no transition points can be found to PDBVT-1 and -2; that is, almost equal correlation intensities are distributed in the whole temperature range.

PCMW can also monitor the spectral variations along the temperature perturbation combining the signs of synchronous and asynchronous spectra by the following rules (in the case of linear increment perturbation): positive synchronous correlation represents increasing spectral intensity; negative represents decreasing; a positive asynchronous correlation can be observed for a convex spectral intensity variation, and a negative one can be observed for a concave variation.³¹ On the basis of this point, from PCMW synchronous spectra, we can obtain the same spectral variations as differential spectra, for example, the number of splitting bands and the variation tendencies at different positions. Similarly, the preference of the band at 1736 cm^{-1} for the columnar phase has also been presented by PCMW synchronous spectra. PCMW asynchronous spectra are usually used to find subtle spectral variations. The PCMW asynchronous spectrum of PDBVT-3 in Figure 4f had been used to determine the mesophase transition temperature regions (70–110 °C) in our previous paper. Although PDBVT-1 and -2 do not show any phase transitions during heating, three or four turning points in PCMW asynchronous spectra could also be easily observed, indicating some subtle carbonyl conformational changes occurred in the amorphous phase.

3.1.4. Two-Dimensional Correlation Spectroscopy. Two-dimensional correlation spectroscopy (2Dcos), first proposed by I. Noda in 1986,^{32,33} can be used to sort out complex or overlapped spectral features and extract additional useful information about molecular motions or conformational changes.

Figure 5 presents the 2Dcos synchronous and asynchronous spectra of three PDBVT samples generated from spectra collected in the mesophase evolving temperature range (70–110 °C). There are two splitting bands at 1736 and 1710 cm^{-1} in the synchronous spectrum of PDBVT-3 (Figure 5 c). The negative cross-peak between these two bands indicates opposite intensity variation tendencies, in conformity with conventional IR analysis results. No apparent splitting bands can be found for PDBVT-1 and -2, except for a strong autopeak (along the diagonal line) around 1716 cm^{-1} . Interestingly, from synchronous spectra, we could also observe the gradually growing band at 1736 cm^{-1} from PDBVT-1 to PDBVT-3, indicating its preference for the columnar phase.

2Dcos asynchronous spectra can significantly enhance the spectral resolution. In Figure 5 d, e, and f, many more splitting bands than those in the synchronous spectra are generated in the asynchronous spectra. For PDBVT-3, four splitting bands at 1707 , 1712 , 1731 , and 1741 cm^{-1} have been identified. Therein, the bands at 1707 and 1712 cm^{-1} should be the splitting bands of the band at 1710 cm^{-1} in the synchronous spectrum, and the bands at 1731 and 1741 cm^{-1} should be those of the band at 1736 cm^{-1} . It is noticeable that these four splitting bands also exist in the asynchronous spectra of PDBVT-1 and -2, which are still in the amorphous phase in the investigated temperature range. It reveals that all the carbonyl conformations corresponding to these splitting bands were coexisting in both the amorphous and columnar phases of PDBVT, with the difference merely lying in the relative concentration of them.

The most important advantage of 2Dcos is its prominent capability to obtain the temporal sequence of events taking place during the studied process. We can deduce the specific orders of these carbonyl splitting bands in the 2D Φ_H phase formation process of PDBVT according to Noda's rule³² as follows (\rightarrow means earlier than): $1731\text{ cm}^{-1} \rightarrow 1741\text{ cm}^{-1} \rightarrow 1707\text{ cm}^{-1} \rightarrow 1712\text{ cm}^{-1}$. The operation details are presented in the Supporting Information. In a sense, this sequence reflects the successive thermal sensitivity of corresponding carbonyl conformations during heating in the mesophase formation temperature range or their contribution ability to the stabilization of the columnar phase. It provides us an important basis for our later assignment of these splitting bands.

It must be pointed out that the 2D correlation patterns in Figure 5c and f are not restricted to PDBVT carbonyl stretching vibrations, but exist in many other carbonyl-containing chemical systems, such as the crystallization process of PLLA¹⁷ and PCL-PEO-PCL triblock copolymer.²⁴ The synchronous spectrum as shown in Figure 5c is called a “four-leaf clover pattern”, and the asynchronous spectrum as shown in Figure 5f is called a “butterfly pattern”. Several spectral simulation reports attributed it to the result of a band position shift combined with a small spectral intensity variation,^{34–37} as we showed in conventional IR spectra in Figure 1. However, in the practical chemical system in this paper, we are devoted to exploring the internal mechanism causing this kind of spectral variations.

3.2. Classification of Carbonyl Conformations of PDBVT. As reported, carbonyl splitting occurs primarily as a result of three coupling formats: via valence bond, via hydrogen bond, and via spacing coupling.¹⁹ Therein, no hydrogen bonding can be formed in PDBVT, which can be excluded first. The spacing coupling arising from electrostatic dipole–dipole interactions or transition dipole coupling certainly contributes to the carbonyl stretching band profile, but it cannot be the dominant factor for three reasons. First, dipole–dipole interactions are observed only in very regular systems (such as the α -crystal of PLLA but not

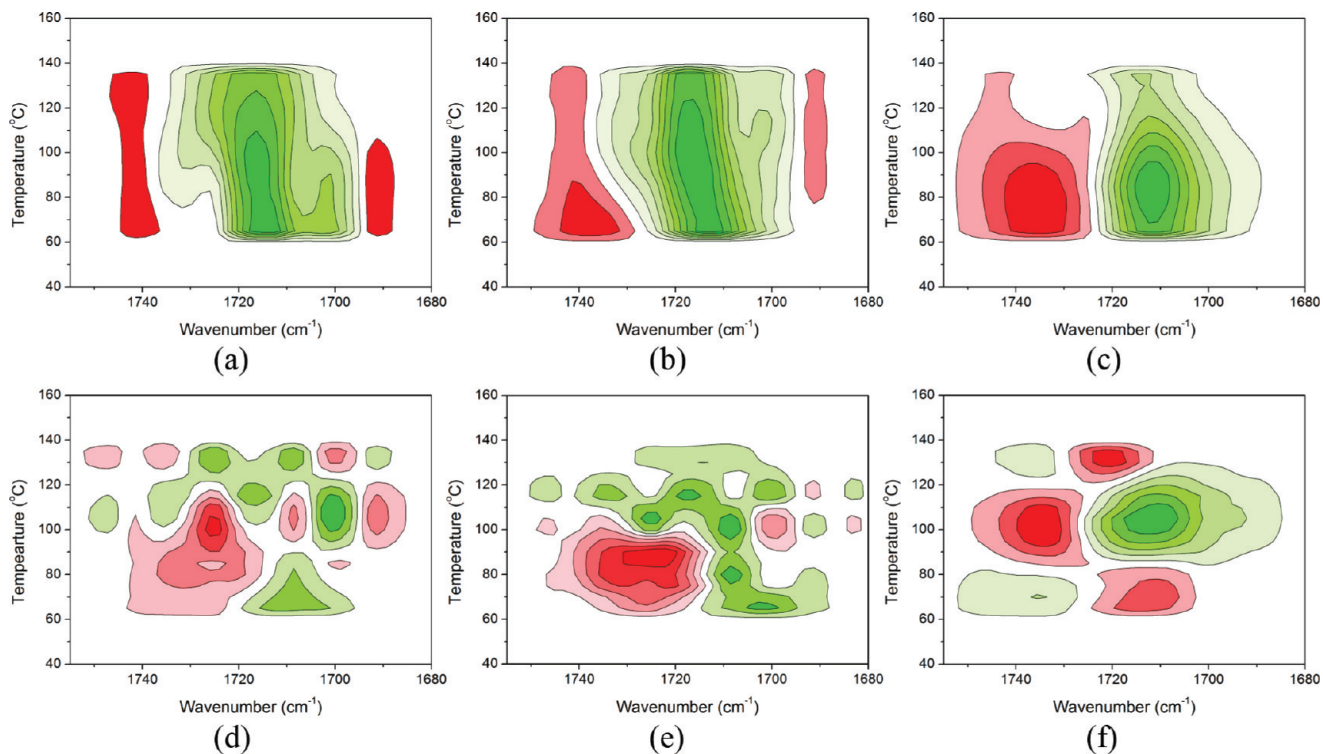


Figure 4. PCMW synchronous and asynchronous spectra of three PDBVT samples generated from the whole spectra during heating (40–160 °C) (synchronous: a, PDBVT-1; b, PDBVT-2; c, PDBVT-3; asynchronous: d, PDBVT-1; e, PDBVT-2; f, PDBVT-3). Red is defined as positive intensities; green, negative intensities.

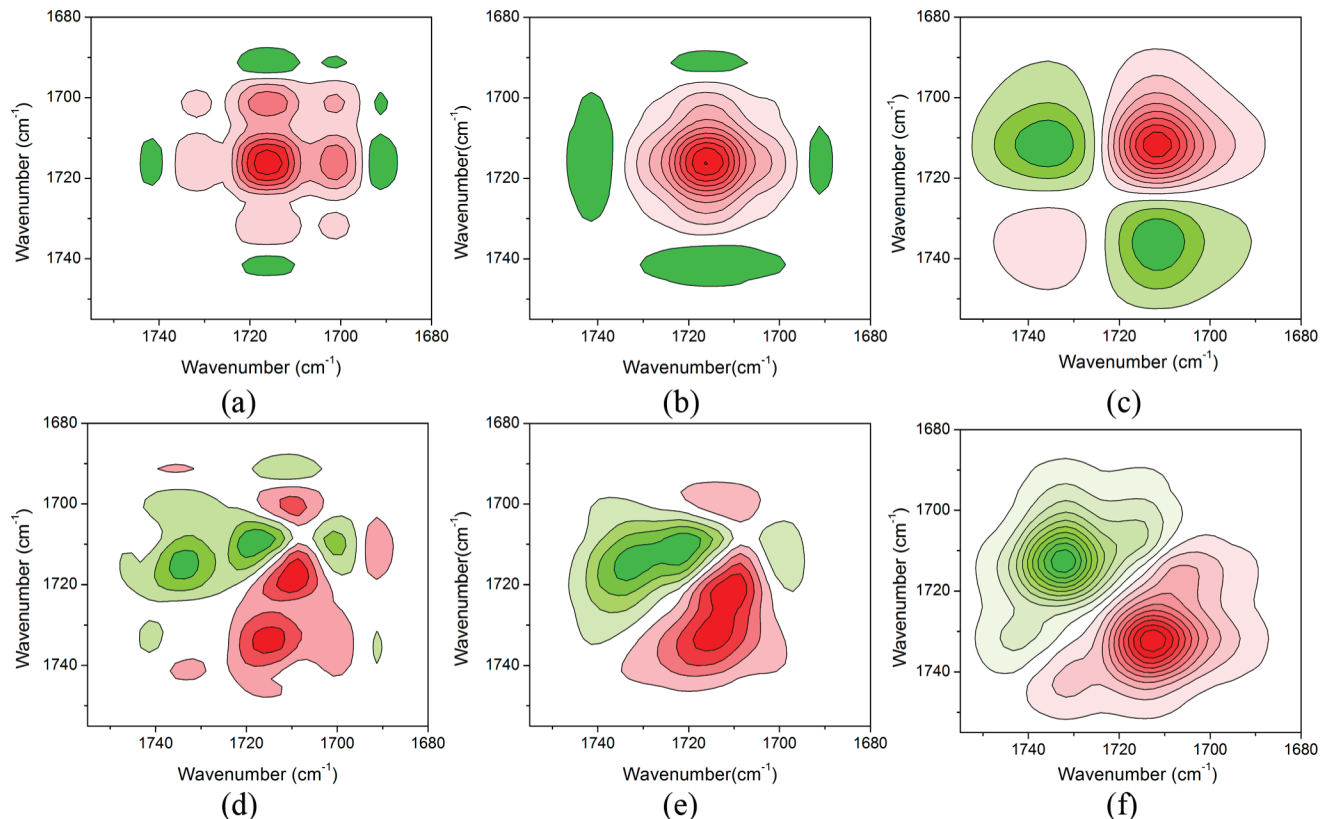
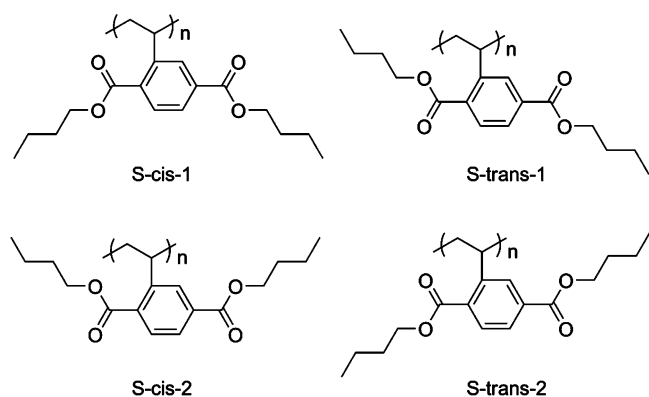


Figure 5. 2Dcos synchronous and asynchronous spectra of three PDBVT samples generated from spectra collected in the temperature range 70–110 °C (synchronous: a, PDBVT-1; b, PDBVT-2; c, PDBVT-3; asynchronous: d, PDBVT-1; e, PDBVT-2; f, PDBVT-3). Red colors are defined as positive intensities; green, negative intensities.

observed in less regular α' crystals¹²). With the columnar phase of PDBVT with a much lower order degree than crystals, it is even harder to show this interaction. Second, even though

dipole–dipole interaction can explain band splitting in ordered arrangement (columnar phase of PDBVT), in the amorphous phase, only band broadening can be expected from dipole–dipole

SCHEME 2: Chemical Structures of PDBVT conformers

interactions because there is a continuum of attractive and repulsive interactions of variable strength, depending on the distance and the orientation between the dipoles.²³ However, a slight peak shift as well as four splitting bands could also be observed in the amorphous phase of PDBVT. Third, on the basis of the above spectral comparison, the frequency of the band preferential to the ordered phase (columnar phase, $\sim 1736\text{ cm}^{-1}$) of PDBVT is higher than that of the band preferential to the disordered phase (amorphous phase, $\sim 1710\text{ cm}^{-1}$), but it is usually the opposite case in hydrogen bonded polymer blends^{38–40} and peptides²⁰ as well as PCL copolymers,²⁴ whose ordered phases are maintained by intermolecular coupling. Thus, it is presumed that carbonyl band splitting of PDBVT might be owing to a kind of intramolecular coupling or valence bond coupling.

Careful observation of the molecular structure of PDBVT shows that the two carbonyls of PDBVT could form a large π -electron resonance system with the neighboring phenylene group. There is no discernible difference in vibrational frequencies between these two carbonyls due to the resonant interaction. As temperature increased, the magnitude of resonance would reduce, leading to the peak of the carbonyl stretching shifting to a higher wavenumber.⁴¹ Thus, we can give a good explanation of the unusual frequency relationship between the columnar and amorphous phases of PDBVT.

It is notable that the resonant interaction between carbonyls and a phenylene group would make them tend to align in a coplanar way. Thus, there are two conformations for each one carbonyl rotating around the single bond. If the side groups of PDBVT are separated from long backbones, carbonyls will rotate more or less freely around the single bond, and the difference in the vibrational energy level between these two conformations is small. However, the substitution of backbone in the ortho and meta positions of the carbonyls differentiates the vibrational energy of the two conformations to a higher extent, then the splitting of carbonyl bands occurs. Similar carbonyl band splitting has also been reported in the ferroelectric liquid crystal system.⁴²

Therefore, we could make a clear classification of carbonyl conformations of PDBVT on the basis of carbonyl rotating in the π -electron resonance system. Scheme 2 shows the molecular structures of PDBVT conformers with four different carbonyl conformations. Their assignment to the four splitting bands will be carried out in the following MD simulation.

3.3. Molecular Dynamics Simulation for PDBVT Conformers. In this part, we will construct four PDBVT conformers with different carbonyl conformations. Both the columnar and amorphous phases were constructed in Materials Studio Visual-

TABLE 2: The Simulated Total Potential Energy of Four PDBVT Conformers

conformers	repeat units	total energy (kcal/mol)	
		helical structures (right handed)	
		right tilted	left tilted
S-cis-1	58.193	63 118	102 603
S-cis-2	57.456	168 161	1 593 573
S-trans-1	57.355	365 889	125 135 543
S-trans-2	57.985	102 511	1 267 637

izer. Due to poor reproducibility of the amorphous phase construction, the potential energy calculation and spectral assignment were performed mainly in the columnar phase. The molecular dynamics run at NVT (constant particle number, volume, and temperature) conditions was also carried out in the amorphous phase to simulate the chain movements of PDBVT.

3.3.1. Construction and Geometry Optimization of Repeat Units. According to the molecular structures of the PDBVT conformers shown in Scheme 2, corresponding repeat units were constructed. The construction details and the final optimized structures are presented in the Supporting Information. The conformational potential energy of four PDBVT conformers has been listed in Table 2. Their stability can be determined in this order: S-trans-1 > S-cis-2 > S-trans-2 > S-cis-1. It is notable that there are no large differences among their conformational potential energies, indicating that without the substitution of a long backbone, the carbonyl can rotate almost freely around a single bond, in accordance with our above-mentioned analysis. In the amorphous phase of PDBVT, the backbones are entangled together with side alkyl chains and do not have apparent influence on the achievement of different carbonyl conformations, so we can use the stability order of repeat units to estimate the relative content of the four conformations in the amorphous phase.

3.3.2. Construction and Potential Energy Calculation of Helical Structures. 2D WAXD results of PDAVTs showed an electron density difference between the center and the outside ring of the columns; that is, the polymer chains adopted a somewhat extended conformation with the cylindrical symmetry.⁴ No experimental observation of the chirality of PDAVT backbones has ever been reported; thus, we often considered it to be a twist conformation. However, in this paper, for the sake of convenience, we still adopted the approximate helical structure of PDBVT backbones for the construction of the columnar phase, and only one column was used for the investigation.

A series of right-handed helical structures of PDBVT with 50 repeat units was constructed, which are presented in Figure 6 from the front and top view of the columns, respectively. The construction details can be also found in the Supporting Information. An obvious difference in density between the center and outside ring could be observed from the top view. To get rid of conformational changes induced by the energy optimization process, no extra dynamics simulation was carried out except for a primary structure relaxation. Their potential energy was calculated by the Discover module based on the COMPASS force field, which is also presented in Table 2.

From the potential energy of different PDBVT conformers, we can obtain their stabilizing effects on the columnar phase. The lower the potential energy, the more stable the helical conformation. Therefore, we determined the sequence of the stabilization of these four PDBVT conformers in the columnar phase as follows: S-cis-1 > S-trans-2 > S-cis-2 > S-trans-1; that

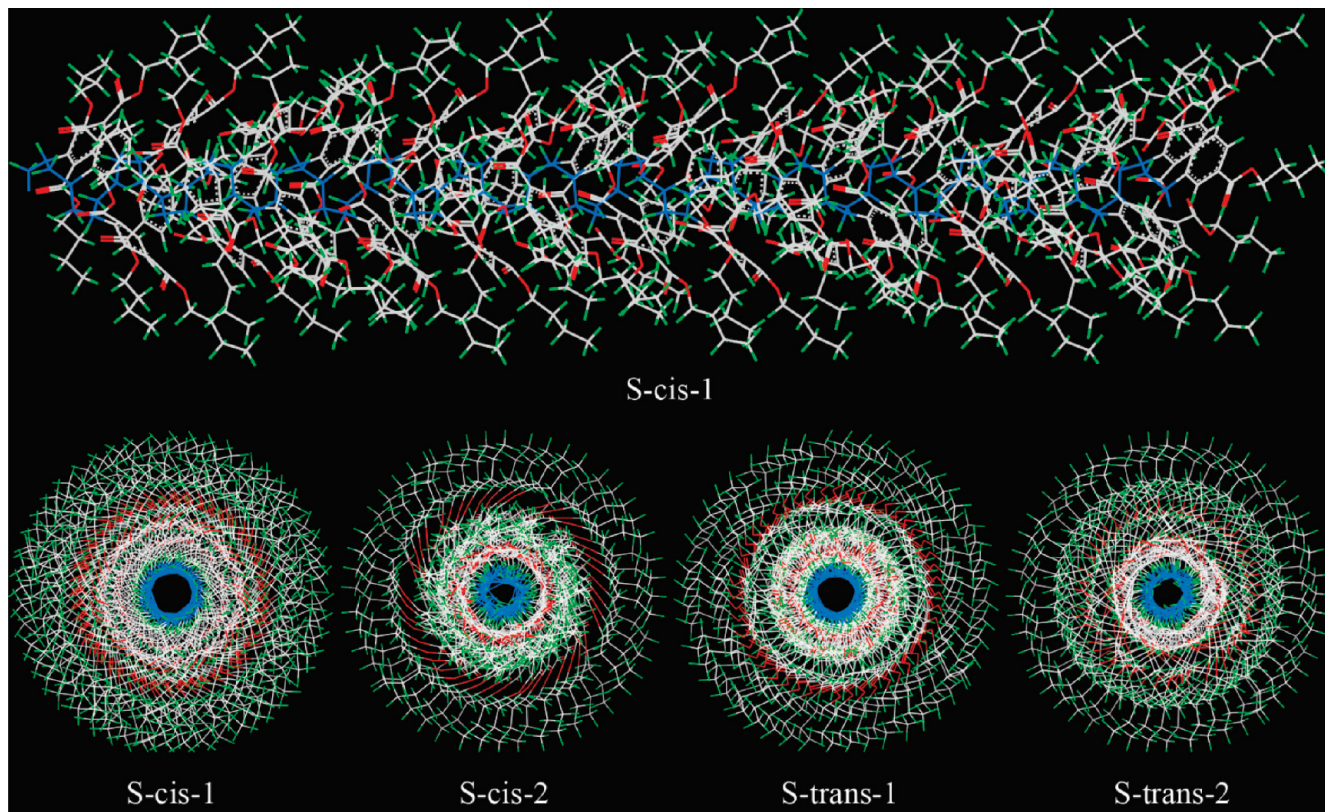


Figure 6. Constructed helical structures (right handed) of different PDBVT conformers from the front view (top, only *S*-cis-1 conformers given) and top view of the columns. Red represents O atoms; green, H atoms; and gray-white, C atoms. Blue represents the backbones.

TABLE 3: Simulated Possible Contributions to Total Potential Energy of Four PDBVT Conformers in the Columnar Phase

conformers	internal ^a	energy (kcal/mol)	vdW ^b	electrostatic	total
<i>S</i> -cis-1	11 418	47 807	893	63 118	
<i>S</i> -cis-2	30 482	136 551	1128	168 161	
<i>S</i> -trans-1	37 378	327 567	944	365 889	
<i>S</i> -trans-2	30 191	71 359	961	102 511	

^a Internal energy arising from the deformation or torsion of bonds and bond angles. ^b Potential energy caused by van der Waals interactions, consisting of repulsive and dispersive interactions.

is, the stabilizing effect of carbonyl at the 2-position (close to backbones) is larger than that at the 5-position (away from the backbones), and the *S*-cis conformation of carbonyls is more stable than the *S*-trans conformation if the conformation of one carbonyl is fixed.

To further understand this order, we listed all the possible contributions to total potential energy in Table 3. It suggests that the *S*-cis-1 conformation has the lowest energy of the three contributions, inducing the total potential energy rather lower than the other three conformations. Although the energy arising from an internal deformation and electrostatic interaction of the *S*-trans-1 conformation is nearly equal to that of *S*-cis-2 and *S*-trans-2 conformations, the large energy arising from van der Waals interactions makes the *S*-trans-1 conformation the most unstable structure to the columnar phase. Of the three contributions to potential energy, that from the electrostatic interaction is very little, indicating the relatively weak dipole–dipole interaction in the low-order columnar phase of PDBVT. The differences among different PDBVT conformers mainly arise from van der Waals interactions or steric hindrance.

We can also observe the steric hindrance of different PDBVT conformers more intuitively from the top view of the column in Figure 6. The large density in the center of the column inevitably results in the instability of the column. It is evidence that the density in the center increases in the order of *S*-cis-1, *S*-trans-2, *S*-cis-2, and *S*-trans-1. The larger density of the *S*-trans conformation than that of the *S*-cis conformation may arise from the more compact contacts due to relatively longer side chains.

3.3.3. Spectral Assignment and Internal Self-Assembly Nature of PDBVT. Combining the spectral comparison (sequence order derived from 2Dcos) and MD simulation results, we can make a clear assignment of the four carbonyl splitting bands: 1707 cm⁻¹, *S*-cis-2; 1712 cm⁻¹, *S*-trans-1; 1731 cm⁻¹, *S*-cis-1; 1741 cm⁻¹, *S*-trans-2. The two splitting bands at 1710 and 1736 cm⁻¹ observed in differential spectra and PCMW synchronous spectra should be the result of carbonyls rotating at the 2-position, whereas the more subtle splitting of them observed in the 2D asynchronous spectra should be the result of carbonyls rotating at the 5-position. The preference of the band at 1736 cm⁻¹ for the columnar phase is due to the relatively stable conformations of *S*-cis-1 and *S*-trans-2. The preference of the band at 1707 cm⁻¹ for the amorphous phase is because the *S*-cis-2 conformation can be achieved much more easily in the amorphous phase than in the columnar phase. Interestingly, if we regard the resonance structure formed by two carbonyls and a middle phenylene as a whole vibrational system, our assignment of *S*-cis and *S*-trans carbonyl conformations is quite similar to that of symmetric and asymmetric stretching vibrations of a three-atom system (such as –CH₂–); that is, the frequency of the *S*-cis carbonyl conformation (symmetric stretching vibration) is lower than that of the *S*-trans carbonyl conformation (asymmetric stretching vibration).

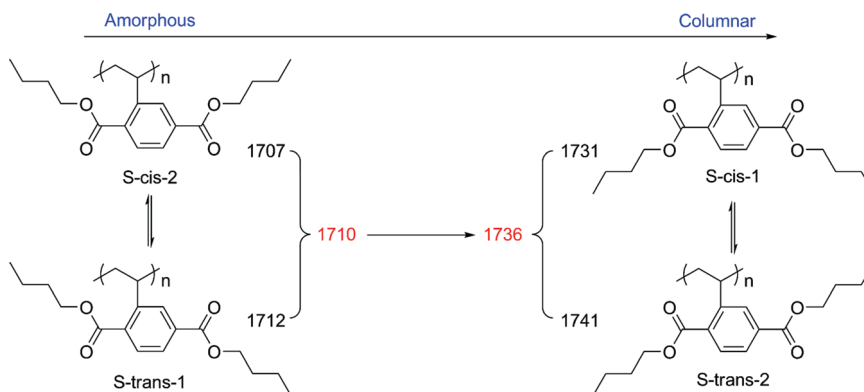


Figure 7. Schematic transformations among different PDBVT conformers in the 2D Φ_H phase formation process and their corresponding spectral assignment.

Compare the stability order of PDBVT conformers in the columnar and amorphous phases (estimated by that of repeat units), and you can find it interesting that the two orders are totally opposite: that is, the conformation stable in the amorphous phase becomes unstable in the columnar phase. It reveals that there exists a transformation process among different carbonyl conformations. Spectral variation tendencies in conventional IR and differential spectra showed that the band at 1736 cm^{-1} had a gradually increasing intensity during heating, but that at 1710 cm^{-1} was gradually decreasing. Therefore, we can deduce the internal self-assembly nature of PDBVT, which can be described as follows: In the amorphous phase of PDBVT, four carbonyl conformations coexisted in the system, with relatively higher content of S-cis-2 and S-trans-1 conformations. As the temperature increased above the mesophase transition point, these two conformations started to transform into S-cis-1 and S-trans-2 conformations through the rotation of carbonyls around the single bond linked to the phenylenes. In other words, the rotation of the carbonyls at the 2-position (close to the backbones) of the phenylenes would take place along with the 2D Φ_H phase formation of the PDBVT. For good comprehension, the schematic transformations among different PDBVT conformers in the 2D Φ_H phase formation process and their corresponding spectral assignment are presented in Figure 7.

As we mentioned above, the stability differences among different PDBVT conformers arise mainly from the van der Waals interaction of bulk side chains. In other words, the transformation of carbonyl conformation should be the result of bulk side alkyl chain movements, but carbonyl had a more rapid and sensitive response to these changes in IR spectroscopy. The movements of side alkyl chains primarily originate from their chain twisting and bending which can be represented by the relative content of trans and gauche conformers. In our simulation results, this part of the contribution to total potential energy was included in the internal energy (as shown in Table 3). It should be noted that the MD simulation of PDBVT conformers in this paper is still rough through simplifying the columnar phase to a virtual ideal model for the convenience of comparison. Recently, a Raman spectroscopic investigation of conformational changes of PDBVT side alkyl chains was carried out in our group, and the thermodynamic parameters of its weak phase transition can also be estimated.

In our previous paper, we deduced the movements of PDBVT backbones from 2DIR results independently, which exhibited “extension–distortion–slight extension” consecutive motions in the whole self-assembly process on the mesoscale.¹⁰ The second process is the key to the formation of the 2D Φ_H phase. To investigate the causality between side alkyl chain movements

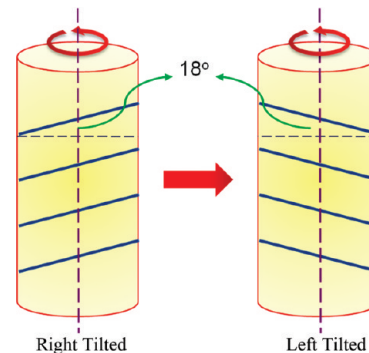


Figure 8. Schematic representation of the construction of PDBVT conformers (left-tilted).

and the distortion of PDBVT backbones, we constructed another four PDBVT conformers with the inclined angle of side chains of -18° , or left-tilted as compared to the right-handed backbones. The schematic representation of the construction of PDBVT conformers (left-tilted) is presented in Figure 8. If the tilted direction of the side chains (or the handed direction of all side chains along the column) is the same as the handed direction of backbones, it should be the side chain movements that induced the distortion of backbones, and vice versa.

The total potential energy of four newly constructed PDBVT conformers is also listed in Table 2. The stabilization order of the four PDBVT conformers (left-tilted) is just the same as that of PDBVT conformers (right-tilted). However, all their potential energy is much higher than that of the PDBVT conformers (right-tilted). In other words, it was the side alkyl chain conformational changes that induced the distortion of PDBVT backbones. This result explained the significant influence of bulk side chains on the formation of the 2D Φ_H phase, which was also consistent with early conjectures about the mesophase formation mechanism of PDAVTs⁴ and MJLCPs.²

3.3.4. Molecular Dynamics Simulation for the Amorphous Phase of PDBVT. As for the first process of PDBVT backbone motions (extending along the polymer main chain axis into a relatively stretched conformation), we could also simulate it by MD simulation. This process occurred in the amorphous phase below the mesophase transition temperature; thus, we used the Amorphous Cell module to construct the amorphous phase first. The representative S-cis-1 conformation was selected to perform the simulation process. The polymer cell was constructed by making a random distributed homopolymer of PDBVT with an orthogonal periodic cell of one chain consisting of 20 repeat units. The constructed structure was geometry-optimized first at 298 K by the Discover module to a realistic density (preset

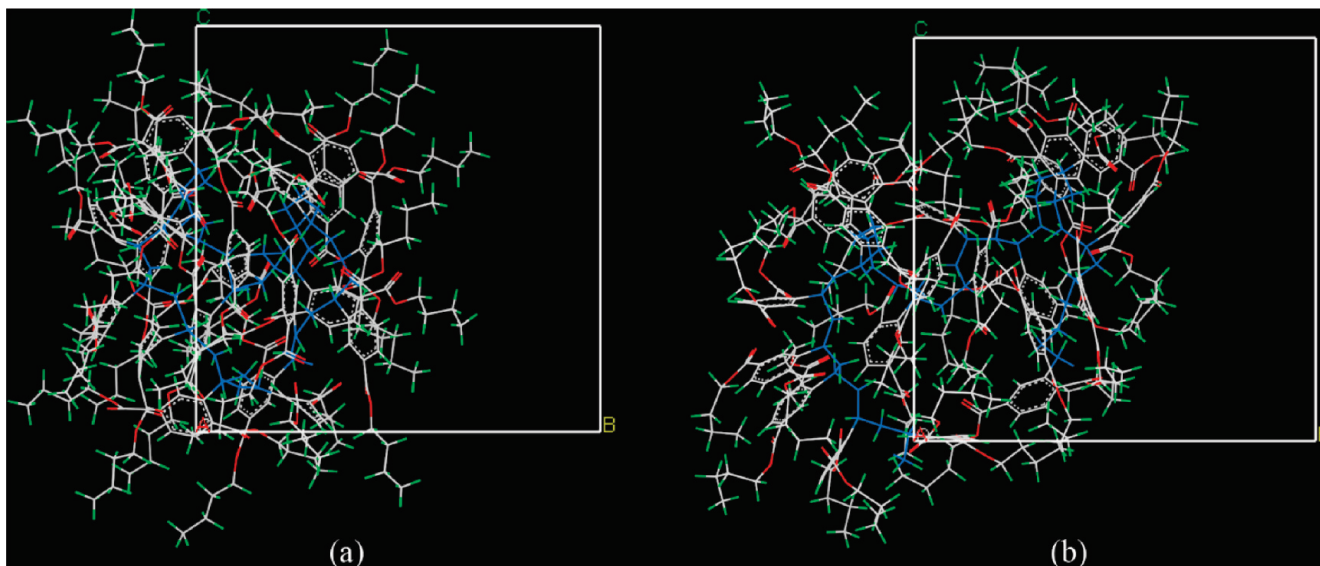


Figure 9. The (a) initial and (b) final structures of PDBVT with *S*-cis-1 conformation in the amorphous phase after molecular dynamics simulation at NVT conditions. Red represents O atoms; green, H atoms; and gray-white, C atoms. Blue represents the backbones.

to 1 g/cm³, according to experimental data (\sim 1.06 g/cm³)²⁸). Then molecular dynamics at NVT conditions (398 K) was carried out for 100 K steps (1 fs each). The initial and final structures are presented in Figure 9.

After a long enough time of molecular dynamics was run at a much higher temperature, PDBVT backbones exhibited an obvious extension, which reproduced the process we proposed on the basis of 2DIR results. The increasing temperature raised the total potential energy of the PDBVT molecules, which tended to release the extra potential energy through the disentanglement of backbones driven by the bulk side chains with improved segmental mobility.

3.4. Molecular Dynamics Simulation for Side Chain Size Dependence of Liquid Crystallinity of PDAVTs. As we mentioned above, PDAVTs could develop into the 2D Φ_H phase only if the linear alkyl groups are in an appropriate range (3–6 carbon chains), and both too short and too long resulted in the disruption of the liquid crystallinity.⁴ In this paper, we attempted to explain this side chain size dependence of the liquid crystallinity of PDAVTs by the MD simulation method.

Each four carbonyl conformations of 12 different repeat units of PDAVTs with different side chain lengths from 1 to 12 were constructed and geometry-optimized by the Discover and Forcite modules, respectively. The operation details were the same as those of the PDBVT and are not described here. The conformational potential energy of each of the 4 carbonyl conformers of these 12 PDAVT repeat units is listed in Table 4. There are also no large differences among the conformational potential energy of the PDAVT conformers of different side chain sizes. For each repeat unit of the different PDAVTs with the side chain all-trans conformation, *S*-cis-2 and *S*-trans-1 conformations are still more stable than *S*-cis-1 and *S*-trans-2 conformations, indicating the more stabilizing effect of a carbonyl at the 2-position than that at the 5-position.

For the convenience of observation, the side alkyl chain length dependence of potential energy of them has been plotted in Figure 10. The $E-m$ curves of four different carbonyl conformers are quite close to each other, and all four curves show about three main changes as the side chain elongates. As the side chain length changes from 1 to 2, a drastic decrease in potential energy occurs due to the length matching of side chains with the repeat chain unit of backbone. As the side chain length changes

TABLE 4: Simulated Potential Energy of Each of the Four Carbonyl Conformers of the 12 PDAVT Repeat Units with Different Side Chain Lengths ($m \sim 1-12$)

PDAVT repeat units	total energy (kcal/mol)			
	<i>S</i> -cis-1	<i>S</i> -cis-2	<i>S</i> -trans-1	<i>S</i> -trans-2
<i>m</i> = 1	63.859	63.516	63.435	63.749
<i>m</i> = 2	49.290	48.693	48.630	49.170
<i>m</i> = 3	58.607	58.041	58.273	58.869
<i>m</i> = 4	58.193	57.456	57.355	57.985
<i>m</i> = 5	59.185	58.246	58.715	59.334
<i>m</i> = 6	62.027	60.852	60.998	61.635
<i>m</i> = 7	61.246	60.328	60.647	60.843
<i>m</i> = 8	63.378	62.721	62.698	63.401
<i>m</i> = 9	65.048	63.901	64.259	64.763
<i>m</i> = 10	66.266	65.233	65.428	66.097
<i>m</i> = 11	67.191	66.056	66.234	66.930
<i>m</i> = 12	69.241	68.154	68.343	69.001

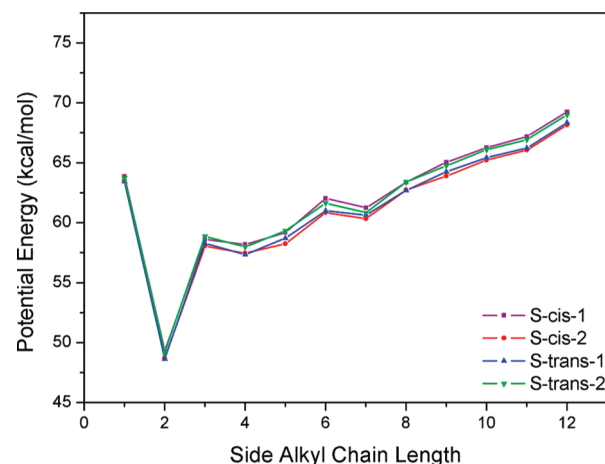


Figure 10. Side alkyl chain length dependence of potential energy of the four carbonyl conformers of PDAVT repeat units.

between 3 and 7, a relatively slight fluctuation of potential energy can be observed. As the side chain length becomes larger than 8, a gradual increase in the potential energy takes place. It is worth noting that the potential energy of PDAVT repeat units reflects the ability of the side chains to maintain the all-trans conformation or, in other words, the “rigidity”. Too short side chains ($m = 1, 2$) surely cannot form any “rigidity”, and too

long side chains ($m = 8\text{--}12$) would also result in the gradual disruption of “rigidity”. Only when the side chain length changes at an appropriate range ($m = 3\text{--}7$) can the PDAVTs form a stable liquid crystallinity. This result is in good conformity with experimental observation (1D WAXD).⁴

4. Conclusion

A combination method of spectral analysis and molecular dynamics (MD) simulation was employed to interpret the carbonyl band splitting phenomenon of PDBVT, a novel thermotropic liquid crystalline polymer, which can self-assemble into the 2D Φ_H phase without conventional mesogens. In our previous paper, 2DIR results showed four splitting bands at 1707, 1712, 1731, and 1741 cm^{-1} ; differential spectra and PCMW exhibited two splitting bands at 1710 and 1736 cm^{-1} . Detailed spectral comparison was carried out with other two PDBVT samples, which cannot form the 2D Φ_H phase with lower molecular weights. It reveals that the band at 1736 cm^{-1} had the great preference for the columnar phase and that at 1707 cm^{-1} , for the amorphous phase.

Four PDBVT conformers were classified according to the carbonyls rotating in a π -electron resonance system. MD simulation for the columnar phase of different PDBVT conformers was performed, and a clear assignment to the four splitting bands was obtained. Then the internal self-assembly nature of PDBVT was deduced, that the rotation of carbonyls at the 2-position (close to backbones) of phenylenes would take place along with the formation of the 2D Φ_H phase.

The self-assembly behavior of PDBVT backbones with “extension–distortion–slight extension” consecutive motions have also been examined by MD simulation. The second process was caused mainly by carbonyl conformation transformations, whereas the first process can be primarily reproduced by the molecular dynamics run of the amorphous phase of PDBVT at NVT conditions.

Finally, the side chain size dependence of PDAVTs was simulated through the comparison of potential energy of their repeat units, which had a good conformity with experimental observation.

Acknowledgment. We gratefully acknowledge the financial support of the National Science Foundation of China (NSFC) (Nos. 20934002, 20774022, 20804010), the Research Program of Education Ministry (No. 200802461016), the National Basic Research Program of China (Nos. 2005CB623800, 2009CB930000). The authors also acknowledge the financial support of the State Key Laboratory for Modification of Chemical Fibers and Polymer Materials, Donghua University.

Supporting Information Available: Additional information as noted in the text. This material is available free of charge via the Internet at <http://pubs.acs.org>.

References and Notes

- (1) Zhou Q. F.; Wang, X. J. *Liquid Crystalline Polymers*; Science Press: Beijing, 1994.
- (2) Zhou, Q. F.; Li, H. M.; Feng, X. D. *Macromolecules* **1987**, *20*, 233.
- (3) Yin, X. Y.; Chen, E. Q.; Wan, X. H.; Zhou, Q. F. *Chin. J. Polym. Sci.* **2003**, *21*, 9.
- (4) Yin, X. Y.; Ye, C.; Ma, X.; Chen, E. Q.; Qi, X. Y.; Duan, X. F.; Wan, X. H.; Cheng, S. Z. D.; Zhou, Q. F. *J. Am. Chem. Soc.* **2003**, *125*, 6854.
- (5) Guan, Y.; Chen, X. F.; Shen, Z. H.; Wan, X. H.; Zhou, Q. F. *Polymer* **2009**, *50*, 936.
- (6) Desper, C. R.; Schneider, N. S. *Macromolecules* **2002**, *9*, 424.
- (7) Papkov, V. S.; Ilina, M. N.; Zhukov, V. P.; Tsvankin, D. Y.; Tur, D. R. *Macromolecules* **2002**, *25*, 2033.
- (8) Molenberg, A.; Möller, M.; Sautter, E. *Prog. Polym. Sci.* **1997**, *22*, 1133.
- (9) Molenberg, A.; Möller, M. *Macromolecules* **1997**, *30*, 8332.
- (10) Sun, S. T.; Tang, H.; Wu, P. Y.; Wan, X. H. *Phys. Chem. Chem. Phys.* **2009**, *11*, 9861.
- (11) Shen, Y.; Chen, E. Q.; Ye, C.; Zhang, H. L.; Wu, P. Y.; Noda, I.; Zhou, Q. F. *J. Phys. Chem. B* **2005**, *109*, 6089.
- (12) Meaurio, E.; Martinez de Arenaza, I.; Lizundia, E.; Sarasua, J. R. *Macromolecules* **2009**, *42*, 5717.
- (13) Aou, K.; Hsu, S. L. *Macromolecules* **2006**, *39*, 3337.
- (14) Meaurio, E.; Zuza, E.; López-Rodríguez, N.; Sarasua, J. R. *J. Phys. Chem. B* **2006**, *110*, 5790.
- (15) Meaurio, E.; López-Rodríguez, N.; Sarasua, J. R. *Macromolecules* **2006**, *39*, 9291.
- (16) Zhang, J. M.; Tsuji, H.; Noda, I.; Ozaki, Y. *J. Phys. Chem. B* **2004**, *108*, 11514.
- (17) Zhang, J. M.; Tsuji, H.; Noda, I.; Ozaki, Y. *Macromolecules* **2004**, *37*, 6433.
- (18) Sarasua, J.-R.; López-Rodríguez, N.; Arraiza, A. L.; Meaurio, E. *Macromolecules* **2005**, *38*, 8362.
- (19) Brauner, J. W.; Flach, C. R.; Mendelsohn, R. *J. Am. Chem. Soc.* **2004**, *127*, 100.
- (20) Bandekar, J.; Krimm, S. *Proc. Natl. Acad. Sci.* **1979**, *76*, 774.
- (21) Bryan, M. A.; Brauner, J. W.; Anderle, G.; Flach, C. R.; Brodsky, B.; Mendelsohn, R. *J. Am. Chem. Soc.* **2007**, *129*, 7877.
- (22) Gorbunov, R.; Stock, G. *Chem. Phys. Lett.* **2007**, *437*, 272.
- (23) Painter, P. C.; Pehlert, G. J.; Hu, Y.; Coleman, M. M. *Macromolecules* **1999**, *32*, 2055.
- (24) Yu, J.; Wu, P. Y. *Polymer* **2007**, *48*, 3477.
- (25) Andersson, S.; Al-Halabi, A.; Kroes, G.; van Dishoeck, E. *J. Chem. Phys.* **2006**, *124*, 064715.
- (26) Lin, Y. C.; Chen, X. *Chem. Phys. Lett.* **2005**, *412*, 322.
- (27) Maus, M.; Wagner, K. G.; Kornherr, A.; Zifferer, G. *Mol. Simul.* **2008**, *34*, 1197.
- (28) Tu, H.; Wan, X.; Liu, Y.; Chen, X.; Zhang, D.; Zhou, Q. F.; Shen, Z.; Ge, J. J.; Jin, S.; Cheng, S. Z. D. *Macromolecules* **2000**, *33*, 6315.
- (29) Mello, C.; Mello, T.; Sevéri, E.; Coelho, L.; Ribeiro, D.; Marangoni, A.; Poppi, R.; Noda, I. *J. Chem. Phys.* **2009**, *131*, 084501.
- (30) Noda, I.; Ozaki, Y. *Two-Dimensional Correlation Spectroscopy: Applications in Vibrational and Optical Spectroscopy*; Wiley: Chichester, 2004.
- (31) Morita, S.; Shinzawa, H.; Noda, I.; Ozaki, Y. *Appl. Spectrosc.* **2006**, *60*, 398.
- (32) Noda, I. *Bull. Am. Phys. Soc.* **1986**, *31*, 520.
- (33) Noda, I. *J. Am. Chem. Soc.* **1989**, *111*, 8116.
- (34) Gericke, A.; Gadaleta, S. J.; Brauner, J. W.; Mendelsohn, R. *Biospectroscopy* **1996**, *2*, 341.
- (35) Czarnecki, M. A. *Appl. Spectrosc.* **1998**, *52*, 1583.
- (36) Czarnecki, M. A. *Appl. Spectrosc.* **2000**, *54*, 986.
- (37) Morita, S.; Shinzawa, H.; Noda, I.; Ozaki, Y. *J. Mol. Struct.* **2006**, *799*, 16.
- (38) Kuo, S. W.; Chang, F. C. *Macromolecules* **2001**, *34*, 5224.
- (39) Motzer, H. R.; Painter, P. C.; Coleman, M. M. *Macromolecules* **2001**, *34*, 8390.
- (40) Huang, H.; Malkov, S.; Coleman, M. M.; Painter, P. C. *Appl. Spectrosc.* **2004**, *58*, 1074.
- (41) Cheng, Y. H.; Wang, X.; Cheng, J. B.; Sun, L.; Xu, W. Q.; Zhao, B. *Spectrochim. Acta, Part A* **2005**, *61*, 905.
- (42) Czarnecki, M.; Katayama, N.; Satoh, M.; Watanabe, T.; Ozaki, Y. *J. Phys. Chem.* **1995**, *99*, 14101.